

Photocurrent Spectroscopy for Quantum-Well Intermixed Photonic Integrated Circuit Design

Gordon B. Morrison, *Member, IEEE*, Erik J. Skogen, *Member, IEEE*, Chad S. Wang, *Student Member, IEEE*, James W. Raring, Yu-Chia Chang, Matt Sysak, and Larry A. Coldren, *Fellow, IEEE*

Abstract—Photocurrent spectroscopy is used to characterize band edges in quantum-well intermixed InGaAsP material lattice matched to InP. The band edge absorption data is used as a design tool to predict the dc performance of electroabsorption modulators, and is shown to agree well with data obtained from actual devices. In addition, we demonstrate the presence of an exciton peak in InGaAsP quantum wells, and present its evolution as a function of quantum-well intermixing and reverse bias voltage.

Index Terms—Electroabsorption modulators (EAMs), excitons, laser tuning, photoconductivity, photodiodes, quantum-well intermixing (QWI), semiconductor lasers.

I. INTRODUCTION

PHOTONIC integrated circuits with monolithic integration of multiple optoelectronic components are highly desirable for next-generation optical networks. Monolithic integration of components such as lasers, electroabsorption modulators (EAM), and passive waveguides, requires multiple band edges. Quantum-well intermixing (QWI) is a popular and simple method for achieving multiple band edges on a single wafer, orthogonal to the growth direction [1]–[4]. The wavelengths of these band edges must be carefully tailored for optimal performance of the integrated photonic circuit. In this letter, we apply band edge photocurrent measurements to the design and performance-analysis of QWI integrated laser modulators. We also present a detailed characterization of the evolution of band edge absorption as a function of the degree of QWI in an InGaAsP quantum well. Photocurrent spectroscopy data for QWI InGaAsP wells have been presented in the literature previously [1], [3], but here we present detailed observation of exciton peaks at multiple biases and with multiple degrees of intermixing. The ability to directly measure the QWI band edge, and to use this measurement for analysis of potential transmitter designs, will enable the engineering of superior

highly optimized integrated laser-modulator transmitters for telecommunications applications [5].

II. FABRICATION

Photodiodes for photocurrent spectroscopy were fabricated from a wafer that initially consisted of seven 65-Å compressively strained quantum wells (conduction band well depth 120 meV) and eight 80-Å barriers sandwiched between two 120-nm waveguide layers grown on InP by metal-organic chemical vapor deposition (MOCVD). This structure was designed for the fabrication of small-footprint chip-to-chip laser-modulator transmitters [4]. A 15-nm InP layer, 20-nm 1.3Q etch stop, and a 450-nm InP implant buffer were grown on top of the waveguide. A 5000-Å SiN_x mask layer was deposited, patterned, and removed in regions where implant was desired. A 100-keV 5e14-cm⁻² dose of P⁺ was implanted into the buffer layer. Rapid thermal annealing at 675 °C was performed to accomplish intermixing [2]. Different levels of intermixing were obtained across the wafer by halting the anneal process and removing the InP implant buffer layer prior to further annealing. By this method, we retained the active (unshifted) band edge, and created three QWI band edges, each blue-shifted by a different amount. The band edges are referred to quantitatively by the wavelengths, in nanometers, of their photoluminescence peaks. The remaining implant layer was removed, and the sample was submitted for MOCVD regrowth of 750 nm of p-type InP above the waveguide, a 750-Å InGaAs contact layer, and a 200-nm InP protective cap.

Each band edge was patterned and etched with circular mesas ranging from 50 to 400 μm in radius. The mesa etch was performed through the waveguide and into the n-type substrate. A 2000-Å layer of SiN_x was deposited by plasma-enhanced chemical vapor deposition, and circular vias were patterned onto the mesas. The protective InP cap was removed, and Ti-Pt-Au ring contacts were deposited. The contacts were annealed at 410 °C for 30 s. Devices were wire bonded to AlN carriers.

III. EXPERIMENT

The wavelength-tunable light source used in our photocurrent measurements is a Varian Cary 500 spectrophotometer. Measurements are taken at 1-nm intervals and the wavelength resolution is 2 nm. An EG&G 5210 lock-in amplifier is used with a 3-kHz chopper and 1-s time constant to extract the photocurrent signal from leakage current. Leakage current for most devices is less than 10 μA at -6 V. A Newport 1835C optical power meter is used to measure the optical power input to the device. An example of data acquired by this method from a 100-μm

Manuscript received August 26, 2004; revised February 17, 2005. This work was supported in part by ARMY Grant DAAD19-03-1-0058. The work of G. B. Morrison was supported in part by an Natural Sciences and Engineering Research Council of Canada (NSERC) PDF.

G. B. Morrison was with the Department of Electrical and Computer Engineering, University of California, Santa Barbara, CA 93106 USA. He is now with III-V Photonics, Houten 3994 DB, The Netherlands (e-mail: tallest_dwarf@hotmail.com).

E. J. Skogen was with the Department of Electrical and Computer Engineering, University of California, Santa Barbara, CA 93106 USA. He is now with Sandia National Laboratories, Albuquerque, NM 87123 USA.

C. S. Wang, J. W. Raring, Y.-C. Chang, M. Sysak, and L. A. Coldren are with the Department of Electrical and Computer Engineering, University of California, Santa Barbara, CA 93106 USA.

Digital Object Identifier 10.1109/LPT.2005.848543

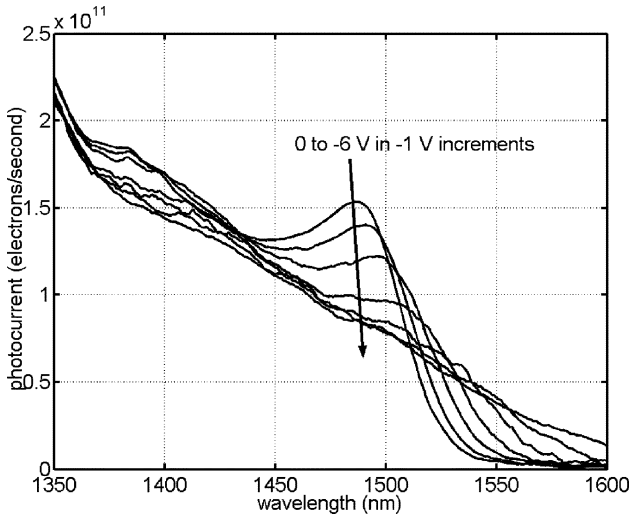


Fig. 1. Photocurrent versus wavelength in device at biases of 0 through -6 V in -1 -V increments.

radius device is shown in Fig. 1. This device was intermixed to approximately 1495 nm from an as-grown band edge of approximately 1540 nm.

The Cary 500 spectrophotometer is useful for calibrating the photocurrent diodes. The absorption of a doped InGaAs contact layer has been determined by measuring transmittance through a 5360 -Å layer grown on undoped InP, and comparing this transmittance to that obtained upon removal of the 5360 -Å layer.

IV. RESULTS AND DISCUSSION

Simple calculations are performed to extract an absorption coefficient from the photocurrent data. Measured incident power is reduced to account for reflection and p-contact absorption. Light incident to the photodiode surface is transverse-electric (TE) polarized. Transverse-magnetic light is not considered because the devices in this letter operate with TE polarization.

Back-scattered light is negligible due to scattering and absorption by the Ti-Pt-Au backside contact. This surprising result was determined by comparing photocurrent magnitude from similar devices on semi-insulating (SI) substrates with and without a Ti-Pt-Au layer annealed on the backside. The magnitudes of photocurrent from doped and SI substrates were the same within experimental error, provided the Ti-Pt-Au layer was annealed on the back side of the SI material. Without the Ti-Pt-Au backside layer, photocurrent is increased by approximately 35% due to back-scattered light.

The measured photocurrent is converted to electrons/second, and each electron is the result of one absorbed photon. Absorption is then obtained as

$$\alpha = \frac{-\ln\left(\frac{P_{in}-P_{out}}{P_{in}}\right)}{L} \quad (1)$$

where P_{in} is the input power in photons per second, P_{out} is the output photocurrent in photons per second, and L is the total length of quantum well material through which the light passes. For these devices, the length was $7 \times 65 \text{ \AA} = 455 \text{ \AA}$.

The absorption data is useful for analyzing device performance. Starting with a spline interpolation of the absorption as

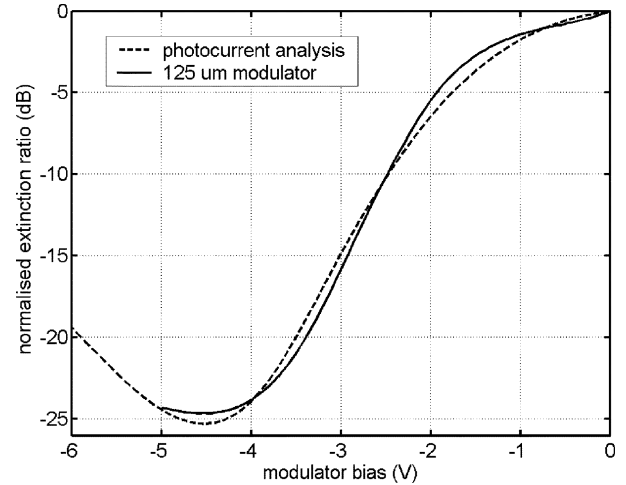


Fig. 2. DC extinction curve for a 125 - μm integrated EAM compared with a simulation using photocurrent spectroscopy data from identical material.

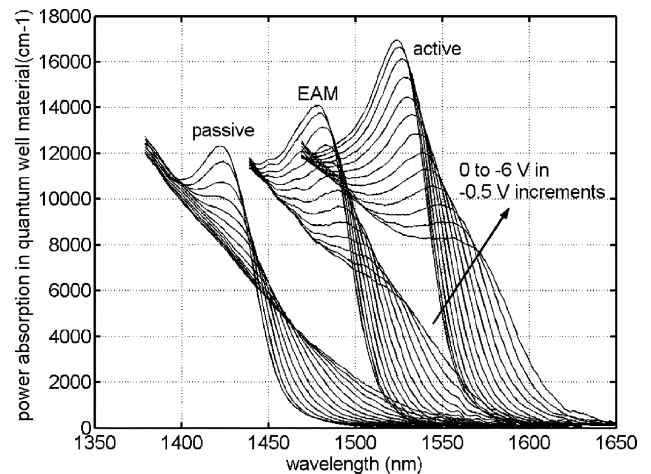


Fig. 3. Active, modulator, and passive absorption edges, obtained by ion-implant QWI. Curves are shown for biases ranging from 0 to -6 V in -0.5 -V increments.

a function of wavelength from data in Fig. 1, simple calculations, which account for optical overlap with the quantum wells and the effective index and length of the waveguide, lead to predicted dc extinction ratios for an EAM. In Fig. 2, the dc extinction of a 125 - μm EAM is simulated at 1542 nm using data from Fig. 1. Also shown for comparison is the dc extinction at 1543 nm of an actual device that was fabricated from the same material intermixed to 1500 nm, and integrated with a 150 - μm distributed Bragg reflector laser [4]. Clearly, the photocurrent measurements allow accurate estimation of modulator performance.

Figs. 1 and 2 demonstrate the useful nature of photocurrent spectroscopy for design of integrated photonic circuits. Of special interest is the strong exciton peak in the QWI InGaAsP material in Fig. 1. The exciton peak is especially important for achieving good dc extinction, as well as negative chirp.

The effect of QWI on the exciton peak is shown in Fig. 3, with band edges for the active, modulator, and passive sections of a photonic integrated circuit. The diodes were biased from 0 to -6 V in -0.5 V increments. The band edges shown in Fig. 3 have photoluminescence peaks at 1537 , 1483 , and 1429 nm. As

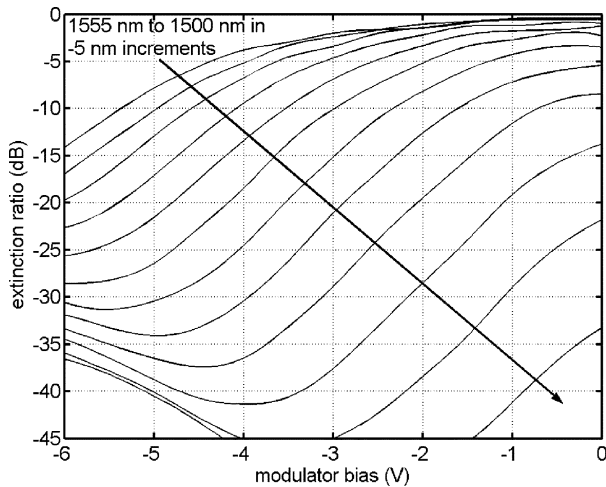


Fig. 4. Predicted dc extinction curves for input light ranging from 1500 to 1555 nm for a 125- μm modulator fabricated from the 1483-nm QWI material of Fig. 3.

the degree of intermixing increases, and the exciton peaks shift to shorter wavelengths, the exciton magnitude decays significantly [3], [6]. With increased intermixing, the exciton peaks also decay more rapidly as a function of applied bias voltage.

The intermixing process results in group V atoms diffusing across the as-grown material boundaries, causing quantum wells to develop rounded edges, and become wider and shallower. This is consistent with the observed behavior of the exciton peaks, which are expected to decay more rapidly with applied voltage when the quantum wells are made shallower by QWI.

In addition to the 1483-nm band edge shown in Fig. 3, there was also a 1460-nm band edge fabricated. These two band edges are both potentially suitable for use in the modulator component of a quantum well intermixed device. In Fig. 4, we compare the simulated dc extinction ratios of 125- μm EAMs operating at wavelengths ranging from 1505 to 1560 nm, using data from the 1483-nm materials. At short wavelengths, the simulated modulator suffers from high insertion loss (high extinction ratio at 0 V), whereas at longer wavelengths, the modulator has a poor extinction ratio. It appears that the ideal operating wavelength for this modulator would be between 1520 and 1540 nm, where extinction ratios larger than 20 dB are obtainable with maximum slopes of up to 10 dB/V, and insertion loss is less than 5 dB.

Simulated dc extinction ratios for EAMs fabricated from the 1460-nm material are shown in Fig. 5. The operating wavelengths are the same as those in Fig. 4, but the 23 nm of additional QWI has a profound effect on the characteristics of the EAM. The performance of the simulated 1460-nm QWI 125- μm modulator is similar to that of the 1483-nm QWI modulator, but the optimal operating point is now at approximately 1500 nm. The maximum extinction ratio obtainable with low (<5 dB) insertion loss is about 20% less for the 1460-nm QWI device, due to reduced carrier confinement caused by increased QWI. A QWI blue shift of about 45 nm is optimal for the structures studied in this letter, and would allow low insertion loss and maximum extinction ratio near the gain peak of the active section of the laser-modulator integrated device. We have reached the same conclusions for QWI InGaAsP wells of different design (80 Å wide, 30% shallower), and thus suggest that 40–50 nm of intermixing is a reasonable criteria that can

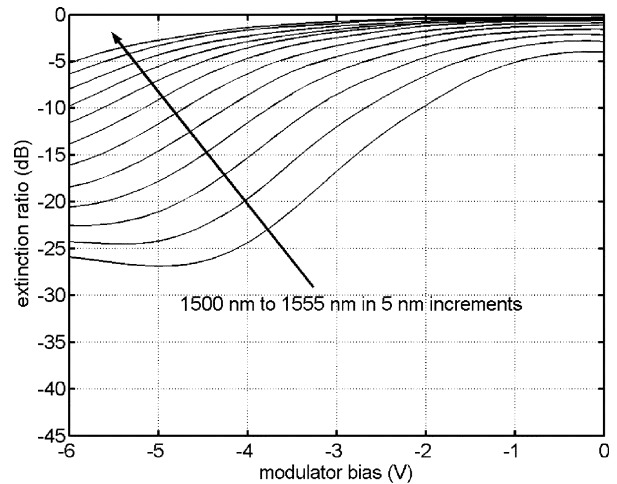


Fig. 5. Predicted dc extinction curves for input light ranging from 1500 to 1555 nm for a 125- μm modulator fabricated from 1460-nm QWI material.

be extended to many different InGaAsP quantum-well designs. Naturally, different results would be expected for very different quantum wells and for quantum wells in other material systems.

V. CONCLUSION

With the advent of QWI as a popular method for monolithic integration of optoelectronic components comes the difficulty of specifically tailoring the various band edges in order to optimize device performance. We have demonstrated that photocurrent data can be exploited to accurately predict extinction ratios for QWI modulators in integrated laser-modulator devices. The influence of QWI on EAM modulator dc extinction ratios at various wavelengths has been presented, and an optimal degree of QWI has been suggested for a range of designs of laser/EAM transmitters in the InGaAsP material system. Photocurrent spectroscopy is an important tool for the engineering of highly optimized photonic integrated circuits.

REFERENCES

- [1] S. Charbonneau, E. S. Koteles, P. J. Poole, J. J. He, G. C. Aers, J. Haysom, M. Buchanan, Y. Feng, A. Delage, F. Yang, M. Davies, R. D. Goldberg, P. G. Piva, and I. V. Mitchell, "Photonic integrated circuits fabricated using ion implantation," *IEEE J. Sel. Topics Quantum Electron.*, vol. 4, no. 4, pp. 772–793, Jul./Aug. 1998.
- [2] E. Skogen, J. Raring, J. Barton, S. DenBaars, and L. Coldren, "Post-growth control of the quantum-well band edge for the monolithic integration of widely-tunable lasers and electroabsorption modulators," *J. Sel. Topics Quantum Electron.*, vol. 9, no. 5, pp. 1183–1190, Sep./Oct. 2003.
- [3] A. Ramdane, P. Krauz, E. V. K. Rao, A. Hamoudi, A. Ougazzaden, D. Robein, A. Gloukhian, and M. Carré, "Monolithic integration of InGaAsP-InP strained layer distributed feedback laser and external modulator by selective quantum-well interdiffusion," *IEEE Photon. Technol. Lett.*, vol. 7, no. 9, pp. 1016–1018, Sep. 1995.
- [4] C. S. Wang, E. J. Skogen, J. W. Raring, G. B. Morrison, and L. A. Coldren, "Short-cavity 1.55 μm DBR lasers integrated with high-speed EAM modulators," presented at the 19th Int. Semiconductor Laser Conf., Matsue-shi, Simane, Japan, 2004.
- [5] T. H. Wood, "Direct measurement of the electric-field-dependent absorption coefficient in GaAs/AlGaAs multiple quantum wells," *Appl. Phys. Lett.*, vol. 48, pp. 1413–1415, 1986.
- [6] J. E. Zucker, K. L. Jones, B. Tell, K. Brown-Goebeler, C. H. Joyner, B. I. Miller, and M. G. Young, "InGaAsP/InP quantum well buried heterostructure waveguides produced by ion implantation," *Electron. Lett.*, vol. 28, pp. 853–855, 1992.